Vol. 76: 131–143, 2018
https://doi.org/10.3354/cr01531

CLIMATE RESEARCH
Clim Res

Published online October 10

Varied degrees of urbanization effects on observed surface air temperature trends in China

Kai Jin[1], Fei Wang[1,2,3,*], Qiang Yu[1,2,3], Jiaojiao Gou[2,3], Huanhuan Liu[4]

[1]Institute of Soil and Water Conservation, Northwest A&F University, Yangling 712100 Shaanxi, PR China
[2]Institute of Soil and Water Conservation, Chinese Academy of Sciences and Ministry of Water Resources, Yangling 712100 Shaanxi, PR China
[3]University of Chinese Academy of Sciences, Beijing 100049, PR China
[4]College of Natural Resources and Environment, Northwest A&F University, Yangling 712100 Shaanxi, PR China

ABSTRACT: Debates over the bias in regional climate records caused by urbanization effects continue, and the diverse estimates of this bias can be partly attributed to different study methods and materials. In this study, we proposed an index (the extent of urban impact, EUI) by quantifying urbanization effects in terms of urban area and station location relative to urbanized areas. The EUI was used to represent the extent of urban impact on the meteorological stations used for observing temperature. Based on the EUI quantification, 569 stations in China were classified into 3 categories: stations with little or no urban impact (R stations), stations with low urban impact (LU stations), and stations with high urban impact (HU stations). Results show that, on average, EUIs for R, LU, and HU stations were 0.3, 2.6, and 15.3%, respectively, implying diverse urbanization influences on the studied stations. Using R stations as a baseline, the average urbanization effects on the warming trend of surface air temperature (SAT) for China during 1961–2012 for the LU and HU stations were estimated to be 0.06 and 0.09°C decade^{-1}, respectively. Therefore, including LU and HU stations to estimate regional SAT trends would lead to notable biases. The bias of the urbanization effect in the average SAT trend of China based on all stations was estimated to be 0.05°C decade^{-1}, accounting for 18% of the overall warming over the period 1961–2012. This estimation should be considered the lowest range of the bias. This study highlights the necessity of considering urbanization effect biases when assessing regional climate change.

KEY WORDS: Surface air temperature · Climate change · Urbanization effect · Station classification · China

1. INTRODUCTION

Cities differ from rural areas in many ways (e.g. extensive impervious surfaces and intensive human activities) and substantially affect the local climate, resulting in an urban heat island (UHI) effect (Heinl et al. 2015). With many regions of the world undergoing rapid urbanization, urbanization biases in surface air temperature (SAT) series have become an issue when meteorological stations located in or close to cities are used to estimate regional temperature change. Previous studies have shown that the effects of urbanization on SAT trends vary at regional and global scales (Jones et al. 1990, Portman 1993, Peterson & Vose 1997, Hansen et al. 2001, Peterson 2003, Ren et al. 2008, 2015, Yang et al. 2013, Wang et al. 2015). These divergences can be attributed to differences in study areas, environmental factors, data used, study periods, and especially analysis methods (Jones et al. 1990, Peterson 2003, Ren & Ren 2011, Y. Li et al. 2013, H. Li et al. 2018a).

The methods for estimating urbanization effects have diversified in recent years and normally include the 'observation data minus reanalysis data

*Corresponding author: wafe@ms.iswc.ac.cn

(OMR)' method (Kalnay & Cai 2003), mathematical models based on some parameters (e.g. population) (Chung et al. 2004, He et al. 2013), and the 'urban minus rural (UMR)' method (Hansen et al. 2001, Peterson 2003, Chen et al. 2006). It has been acknowledged that each method has its limitations, and different methods may give different results. For example, most satellite data and reanalysis products have relatively short time series for UHI studies. In addition, although reanalysis data are not sensitive to urbanization or land-use effects (Kalnay & Cai 2003), some factors, such as changes in cloud cover and surface moisture, have been excluded from the climate models used in the data assimilation, which may bias the UHI assessment (Trenberth 2004). The parameter-based mathematical method can only be applied if there are enough stations with varying degrees of urbanization to represent regional averages (Karl et al. 1988). In general, the UMR method is one of the most popular and reliable methods and can be used at various scales (Peterson 2003, Li et al. 2004b, Ren et al. 2008, Wang et al. 2015).

Classifying meteorological stations into different categories (e.g. urban, suburban, and rural) is a key procedure in the UMR method (Ren & Ren 2011). In general, the nearest rural stations are directly selected without specific criteria in local-scale studies (Tayanç & Toros 1997, Xiong et al. 2010). Regional studies often employ population data, large-scale maps, energy consumption, or land use/land cover data to categorize stations, but the thresholds are inconsistent or contentious (Portman 1993, Li et al. 2004b, Hua et al. 2008, Mohsin & Gough 2012, Li et al. 2013). A few previous studies even adopted a comprehensive procedure considering several of the factors mentioned above to investigate urbanization biases (e.g. Zhang et al. 2010). However, their processes required large amounts of metadata and several thresholds for selecting reference stations (Ren et al. 2015). In another approach, classification is conducted by identifying station locations in isothermal maps based on SAT (Winkler et al. 1981), but this method is more applicable for local-scale studies because of the complicated process of manual identification (Ren & Ren 2011). Moreover, nighttime stable light (NSL) data have been used to categorize stations (Owen et al. 1998, Hansen et al. 2001). Although this method is limited in its comparability among different countries, cultures, and economic regions (Liu et al. 2012), it is a simpler and faster method than the other above-mentioned methods. Therefore, if optimal thresholds for extracting urban areas from different regions can be found, NSL data can be well applied at large scales.

Another important issue in quantifying the impacts of UHI is related to city size (Li et al. 2018b) and station location (Jin et al. 2015). Population size (Karl et al. 1988) and urban area (Zhou et al. 2014) are positively correlated with the magnitude of the UHI effect. Moreover, the impact of UHI on temperature decreases with increasing distance from the station to the city center (Khandelwal et al. 2011, Heldens et al. 2013). Previous studies often considered the station location using the threshold of a fixed distance, and rarely quantified the gradual reductive impact of UHI based on changes in distance (e.g. Yang et al. 2013). If we do not consider this impact, we might select different rural stations, which would result in the estimation of the urbanization bias deviating from the real magnitude (Jones & Lister 2009, Ge et al. 2013). For instance, using different rural stations, Mohsin & Gough (2012) showed that the estimated trends for the UHI intensity at the 'Toronto downtown' station and the 'Toronto Pearson' station ranged from 0.01 to 0.02°C decade^{-1} and from 0.03 to 0.035°C decade^{-1}, respectively.

Here we aimed to properly describe urbanization effects over China by considering urban areas and station locations relative to urbanized areas with the help of a new index, termed the extent of urban impact (EUI). The EUI index is used to represent the extent of the urban impact on meteorological stations for temperature observation. Compared with previous indexes, such as surface imperviousness (Li et al. 2018b), urban fraction (Li et al. 2017, Wang et al. 2017), and population (Karl et al. 1988), EUI is a more integrated index for reflecting the urban impact and incorporates information of UHI intensity and its impact on stations related to different distances. Based on EUI, 569 stations in China were classified into 3 categories: stations with little or no urban impact (R stations), stations with low urban impact (LU stations), and stations with high urban impact (HU stations). Urbanization biases in SAT series were calculated by analyzing the difference in regional average SAT trends between R stations and other station groups. The method described here and its results can be used as a reference for detecting urbanization effects in the observed SAT trends over China. The rest of this paper is organized as follows. In Section 2, we describe the data and methods used, and we analyze the results in Section 3. In Section 4 we discuss several of the important issues used for drawing our conclusions, which are summarized in Section 5.

2. METHODS

2.1. Temperature data and homogeneity adjustment

In this study, we selected 569 national basic/reference surface stations located in mainland China with temperature records from 1961–2012 (Fig. 1). The SAT data, mainly including the China Homogenized Historical Temperature (CHHT) (1961–2004) dataset (Li et al. 2004a), were obtained from the China Meteorological Data Service Center (http://data.cma.cn/en). The CHHT is a homogenized dataset that has been adjusted for inhomogeneities mainly relating to station relocation based on the Easterling–Peterson technique (Easterling & Peterson 1995, Li et al. 2004a). In this study, we updated the SAT series to include data up to 2012 by connecting historical SAT records (2005–2012) to the CHHT series (1961–2004) (Ren & Zhou 2014). Then, according to the method proposed by Li et al. (2004a), the connected SAT series of the stations that were relocated after 2004 was adjusted for inhomogeneities. After connection, rechecking, and adjustment, the homogeneities and continuities of the SAT series during 1961–2012 were comparatively reasonable. A detailed explanation of this procedure is given in Fig. A1 in the Appendix.

2.2. Regionalization of the SAT series

A recent study suggested that surface UHI intensity was affected by the inter-annual background climate variability (Yao et al. 2017). This implies that urbanization effects on SAT trends may vary within a large-scale region because of inter-annual temperature change. Therefore, to analyze the potential difference in urbanization effects among different regions, we divided China into several sub-regions based on the inter-annual temperature change of the meteorological stations. Based on Li et al. (2004b), rotated principal component analysis (RPCA) (Horel 1981) was applied to divide China into sub-regions based on the annual mean temperature of all stations from 1961–2012. Two main steps were taken. First, principal component analysis (PCA) was used to reduce the variability in the 569 SAT series into a few

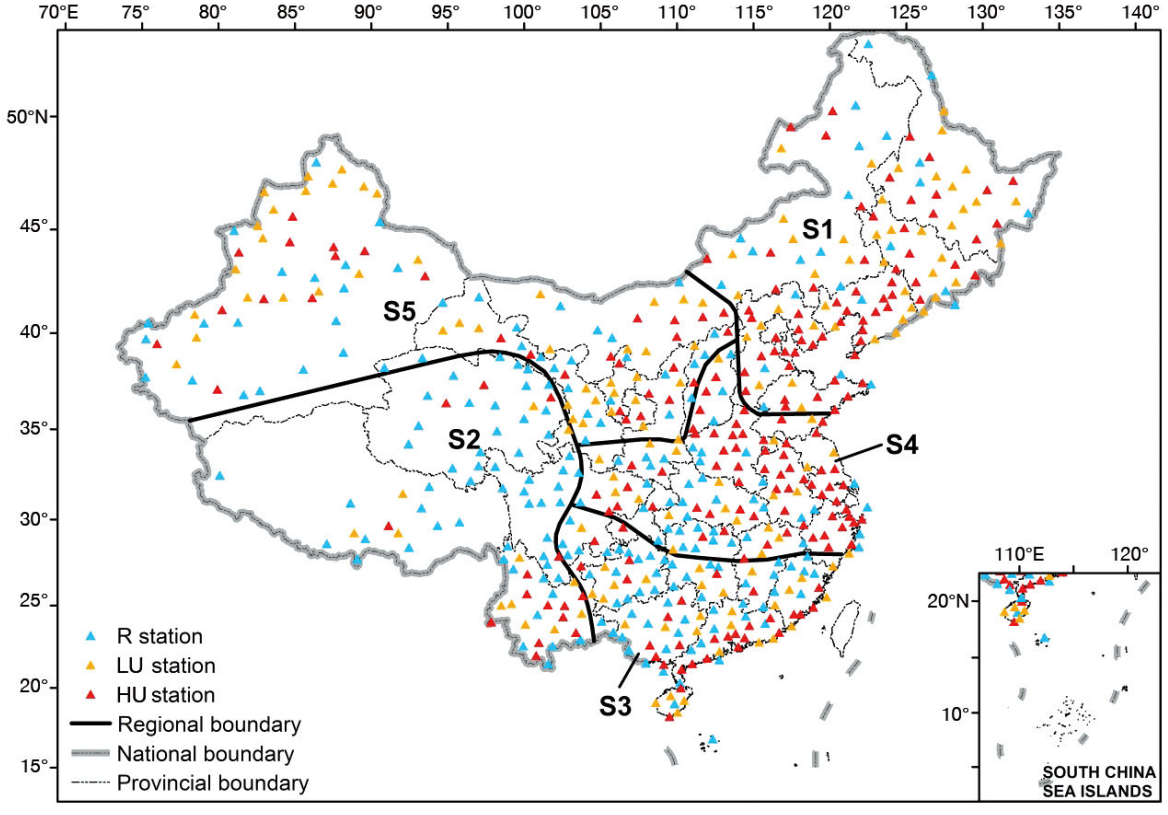

Fig. 1. Distributions of the 5 sub-regions for the surface air temperature (SAT) series and the 569 meteorological stations over China (S1–S5 indicate the first–fifth sub-regions, respectively). R, LU, and HU stations are stations with little or no urban impact, with low urban impact, and with high urban impact, respectively

Table 1. Variance contribution rates and cumulative variance contribution rates of the 7 principal components (PC); RPC: rotated principal component

	1	2	3	4	5	6	7
PC							
Variance contributions (%)	65.12	9.93	5.65	3.09	2.36	2.19	1.66
Cumulative contributions (%)	65.12	75.05	80.70	83.79	86.15	88.34	90.00
RPC							
Variance contributions (%)	23.55	17.25	16.68	16.12	12.55	2.79	1.06
Cumulative contributions (%)	23.55	40.8	57.48	73.6	86.15	88.94	90.00

principal components (PCs), i.e. weighted linear combinations of the original variables. In this study, the first 7 PCs (i.e. PC1–PC7) contained 90% of the cumulative variance contribution, implying that they could well explain the total variance of the original data (Table 1). Second, the loadings of the 7 PCs were used to conduct a varimax rotation, which could better reflect the local difference of the original variables (Kaiser 1958, Li et al. 2004b). The rotated PC (RPC) refers to a linear transformation of the initial PCs (Horel 1981). After rotation, the variance contributions of the first 5 RPCs (i.e. RPC1–RPC5) were above 10%, with a cumulative variance contribution of up to 86.15% (Table 1). Based on the rotated loadings of RPCs (loading values above 0.5), meteorological stations with geographical contiguity were classified as belonging to the same sub-regions (Fig. 1). The detailed calculations of the RPCA and the varimax method can be found in Kaiser (1958).

2.3. Classification of meteorological stations

In this study, meteorological stations of China were classified into 3 groups based on the EUI, which was quantified by considering urban areas and the distance from urbanized area to station. The China City Yearbook 2012, which contains the data of urban built-up areas, was obtained from the National Bureau of Statistics of China (www.stats.gov.cn). In addition, the NSL data from the Defense Meteorological Satellite Program's Operational Line-scan System (DMSP/OLS) were obtained from the US National Geophysical Data Center (NGDC) (https://ngdc.noaa.gov/eog/download.html). The digital number (DN) value of each pixel was the average of the visible-band DN values of lights from cities, towns, and other sites with persistent lighting. The values of NSL data range between 0 and 63, including background noise with the value of 0 and lit pixels with values of 1–63. With a resolution of 1 km, DMSP/OLS NSL data have been frequently used to extract information about urban expansion at regional and global scales (Imhoff et al. 1997, Liu et al. 2012). The empirical threshold-based approach is one of the most popular methods for the extraction of urban areas (Jin et al. 2018). However, because of the 'diffuse lighting' phenomenon in densely populated areas (Elvidge et al. 1999), the optimal thresholds of NSL should be based on the regional economic or urbanization levels (Liu et al. 2012). For example, Liu et al. (2012) extracted urban areas of 8 economic regions in China in 2005, with different thresholds in the range 38–60 DN. Jin et al. (2018) extracted urban areas with different thresholds in the range 35–55 for the 71 largest cities of China. Based on the data of urban built-up areas, we first classified the cities and towns into 3 groups (large, medium, and small cities). Then, based on Jin et al. (2018), urban areas were extracted with the different thresholds of NSL using ArcGIS 10.0 (Table 2).

Li et al. (2013) adopted a weighted ratio of effective energy consumption pixels in 3 circular buffer zones to reflect the impact of energy consumption on a meteorological station. Similarly, urban impact on stations can be represented by a weighted ratio of the urban area near the station. Based on Li et al. (2013), 3 circular buffer areas with radii of 10, 20, and 30 km at each station were drawn in ArcGIS 10.0. The areas near the stations were then divided into 3 subzones (Zones a, b, and c) (Fig. 2). Urban areas in the 3 subzones were counted using ArcGIS 10.0 to quantify the EUI. According to Jin et al. (2015), EUI is defined as the extent of urban impact on meteorological stations for temperature observation, which can be calculated by Eqs. (1) & (2):

Table 2. City size categories and the corresponding thresholds of nighttime stable light (NSL) data in China for 2012. The different thresholds of NSL data were determined based on the study of Jin et al. (2018) and are given as digital numbers

Size category	Built-up area of city (km^2)	Number of cities	Threshold of NSL data
Large cities	>100	92	55
Medium-size cities	50–100	106	45
Small cities and towns	<50	90	35

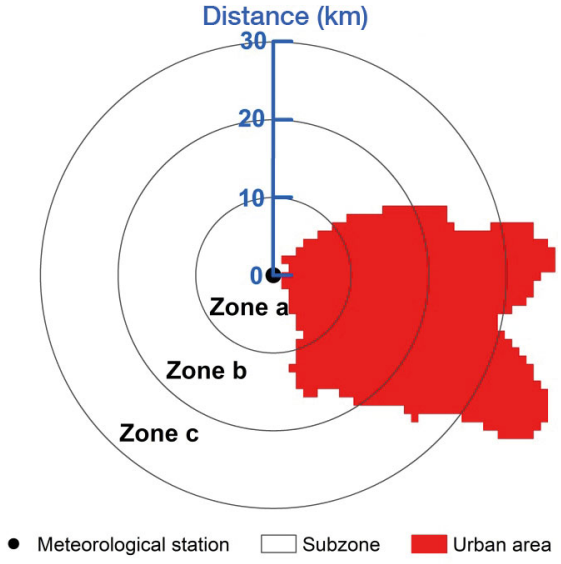

Fig. 2. Sketch of subzones and urban areas close to meteorological stations using the example of Wuhan City

$$\mathrm{EUI} = \frac{K}{K_0} \times 100\% \quad (1)$$

$$K = \frac{S_a}{R_a} + \frac{S_b}{R_b} + \frac{S_c}{R_c} \quad (2)$$

where S_a, S_b, and S_c are the urban areas in Zones a, b, and c, respectively, in km^2; R_a, R_b, and R_c are the radii of the circular buffer areas, namely the distances from the station to the boundary of Zones a, b, and c, respectively (R_a = 10 km, R_b = 20 km, and R_c = 30 km); and K and K_0 are the actual and maximum values, respectively. K_0 was calculated with S_a, S_b, and S_c equaling the areas of Zones a, b, and c, respectively.

To guarantee a sufficient number of reference stations, especially in East China, previous studies used a relatively relaxed standard for station classification (Li et al. 2004b, Ren et al. 2008, 2015). In general, the thresholds of station classification were determined by an empirical method. For example, Wang & Ge (2012) selected those stations with the least urban land-use expansion (<100 ha) as reference stations. Similarly, the 569 meteorological stations were classified into 3 categories based on the empirical method and the values of EUI: a station with little or no urban impact (EUI < 1%, R station), a station with low urban impact (1% ≤ EUI < 5%, LU station), and a station with high urban impact (EUI ≥ 5%, HU station). An R station is a rural or reference station with negligible urban effects. LU and HU stations are urban stations with urbanization effects. Owing to the higher urbanization level and population density in East China, we selected R stations with EUI < 2% in Jilin, Liaoning, Hebei, Henan, Shandong, Anhui, and Jiangsu provinces. The selection criterion of LU stations in these provinces was 2% ≤ EUI < 5%.

2.4. Estimation of temperature change and urbanization effects

Based on the annual mean SAT data of 569 stations, we first calculated the annual mean SAT anomalies for each station over the period 1961–2012. The reference period used was 1971–2000. SAT anomalies of the stations within each 5° × 5° latitude–longitude grid were then averaged to obtain the mean SAT anomalies of the grids (Fig. 1). Finally, the average SAT anomaly series based on each station group were generated for the sub-regions and China as a whole using the grid area as the weighting coefficient (Jones & Hulme 1996). To ensure the uniformity of station distribution, based on the study of Ren & Zhou (2014), we only analyzed those grids including at least 1 reference station (R station) and 1 urban station (LU or HU station). Thus, 46 grids in the study region were analyzed. The 5 grids that had only reference stations were all located along national boundaries or in Southwest China.

Spatial and temporal variations in the annual mean SAT over China during 1961–2012 were analyzed based on the linear trends of SAT anomalies of 569 stations and the Kriging method (Holdaway 1996). We assumed that the effects of urbanization on temperature trends of R stations could be neglected. Thus, the urbanization effects ($\Delta Trend$) were calculated by analyzing the difference in regional average temperature trends between R stations and other station groups (i.e. LU, HU, and all national stations) (Ren et al. 2008, Zhang et al. 2010, Zhou & Ren 2011). $Trend_R$, $Trend_{LU}$, $Trend_{HU}$, and $Trend_T$ indicate the trends of the regional average SAT anomaly series based on R, LU, HU, and all stations, respectively, and were calculated by the least-squares method (Li et al. 2004b). Based on Zhang et al. (2010) and Ren et al. (2008), the contribution of urbanization warming to the overall trend of regional average SAT series (urbanization contribution, C) was calculated as follows:

$$\Delta Trend = Trend - Trend_R \quad (3)$$

$$C = \frac{\Delta Trend}{Trend} \times 100\% \quad (4)$$

where $\Delta Trend$ indicates the difference in trends of the regional average SAT series between the refer-

ence stations and other station groups (i.e. LU, HU, and all stations); that is, the urbanization effect (Ren et al. 2008), in °C decade^{-1}; *Trend* indicates the overall trend of the regional average SAT series based on LU, HU, or all stations ($Trend_{LU}$, $Trend_{HU}$, or $Trend_{T}$), in °C decade^{-1}; $Trend_{R}$ indicates the trend of the regional average SAT series based on the reference stations, in °C decade^{-1}; and C is considered 100% when $\Delta Trend$ is larger than $Trend_{LU}$, $Trend_{HU}$, or $Trend_{T}$ (Zhang et al. 2010).

3. RELULTS

3.1. RPCA sub-regions and station classification

The first and second sub-regions (S1 and S2) were Northeast China and Southwest China, respectively (Fig. 1). Sub-region S3 was South China. Sub-region S4 included East, Central, and part of North China, and S5 covered all of Northwest China and part of North China. In addition, each sub-region included about 100 meteorological stations, except for S2, which had 82 meteorological stations. Overall, our results of RPCA sub-regions were consistent with the division given by Li et al. (2004b) based on 390 stations. There was only 1 obvious difference: a part of South China included in S3 in our division was classified into another sub-region in the division by Li et al. (2004b). This is mainly related to differences in the number of meteorological stations and the length of SAT time series used.

The classification result showed that there were 219 R stations with an average EUI of 0.3%, 150 LU stations with an average EUI of 2.6%, and 200 HU stations with an average EUI of 15.3% (Table 3). However, station distribution in different categories varied by region. The number of R stations in Southwest China and part of South China was far greater than in Northeast China and the coastal areas of East China. Furthermore, in Southwest China (S2), there were only 12 LU stations and 15 HU stations, but 55 R stations. The average values of EUI in West and South China (S2, S5, and S3) were significantly lower than in East China (S1 and S4). Beijing station, located in S1, had the largest EUI, which was calculated to be 71%. The unbalanced distribution of stations and different EUI in different sub-regions can be partly attributed to the difference in regional economy and urbanization levels. Therefore, regionalization of SAT series over China is useful for analyzing the differences in temperature changes between rural and urban stations.

3.2. Spatio-temporal variation of SAT

The distribution of annual mean SAT changes over China showed clear regional differences (Fig. 3). Most regions of China showed a warming trend, with the rate being higher than 0.1°C decade^{-1} during 1961–2012, except for a small area of Central China. Moreover, there were some 'islands' in which temperatures increased more rapidly than temperatures in their surrounding areas. For instance, the Yangtze Delta area, located in the coastal area of East China, presented greater warming than nearby areas. The Yangtze Delta area includes several large and medium cities that are economically developed and densely populated, such as Shanghai. Therefore, the severe impact of urbanization on temperature change may be one of the reasons for local warming.

We calculated the average trends of each sub-region during 1961–2012 (Table 3). All sub-regions showed significant warming ($p < 0.01$), and their SAT trends were obviously different. The average temperature of S5 had the highest increase, with a trend of 0.353°C decade^{-1}. In contrast, the average temperature of S3 increased with a trend of 0.183°C decade^{-1}. The average trend of SAT over China was 0.285°C decade^{-1} ($p < 0.01$). The regions identified to exhibit significant warming in China matched well with

Table 3. Number and average extent of urban impact (EUI, %) of different station groups and the regional average temperature trends in different sub-regions and China. S1–S5: first–fifth sub-region. R, LU, and HU stations: stations with little or no urban impact, low urban impact, and high urban impact, respectively. Temperature trend: trend of regional average surface air temperature (SAT) anomaly series during 1961–2012 (°C decade^{-1}). $^{**}p \leq 0.01$ (significance determined using a *t*-test)

Region	R station		LU station		HU station		Total		Temperature
	Number	EUI	Number	EUI	Number	EUI	Number	EUI	trend
S1	24	0.9	44	3.0	62	16.7	130	9.1	0.345**
S2	55	0.1	12	2.1	15	10.1	82	2.2	0.293**
S3	56	0.1	29	2.6	30	15.1	115	4.6	0.183**
S4	40	0.4	22	2.9	63	15.6	125	8.5	0.224**
S5	43	0.3	44	2.2	30	14.7	117	4.7	0.353**
China	219	0.3	150	2.6	200	15.3	569	6.2	0.285**

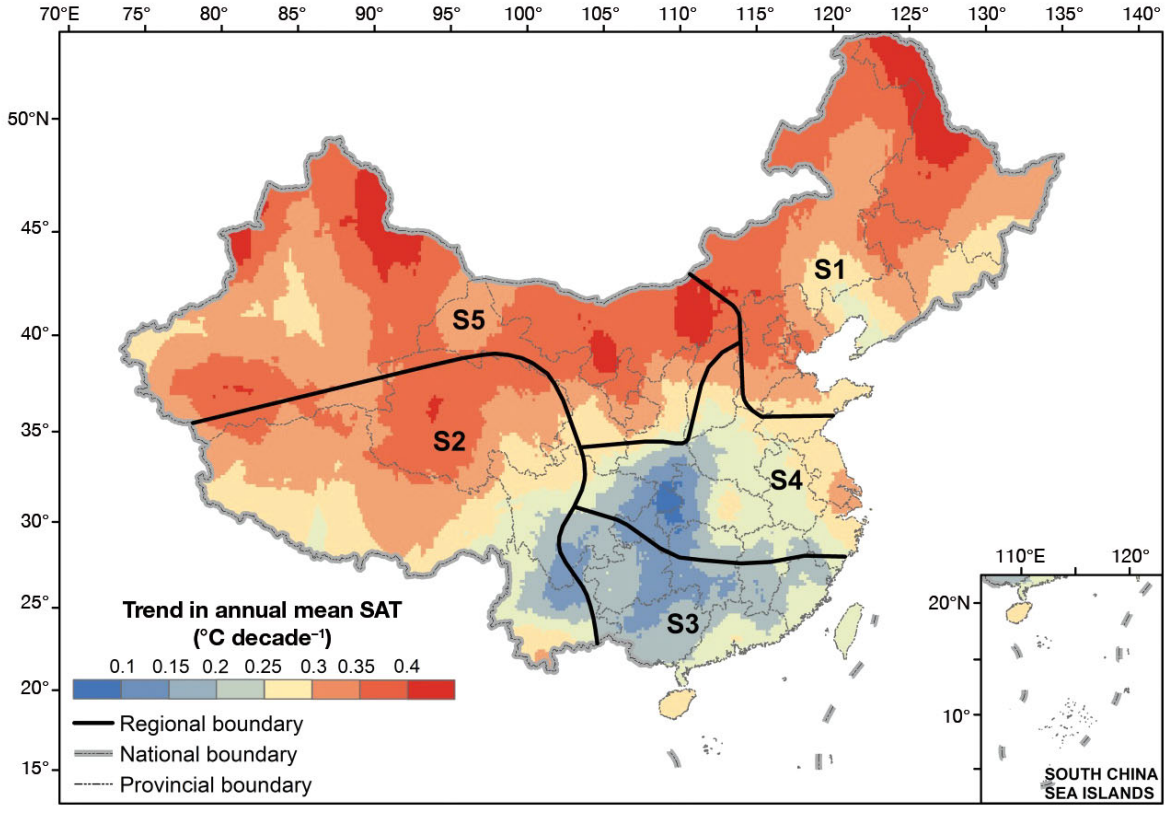

Fig. 3. Spatiotemporal variation of annual mean surface air temperature (SAT) anomalies over China during 1961–2012

the result of the IPCC Fifth Assessment Report (AR5) related to global warming (Hartmann et al. 2013). However, the difference in inter-annual temperature change among the 5 sub-regions may enhance the diversity of urbanization effects on observed SAT trends in China (Yao et al. 2017).

3.3. Urbanization biases in the SAT series

Fig. 4 shows the temporal variation for average SAT anomalies of R stations and all national stations over China during 1961–2012. The average SAT anomalies of R stations and all national stations of China showed a significant positive trend. However, the trend rate of the annual mean SAT series based on the national stations was larger than the trend rate based on R stations. Because of the historical and unique socio-economic conditions, most of the national stations were positioned in or close to cities (Ren et al. 2008). In the past several decades, China has undergone rapid urbanization, with the urban population increasing from 0.54 billion in 1949 to 1.35 billion in 2012, implying a higher warming trend for urban stations than rural stations (Ren et al. 2015). The annual mean SAT trends for R stations and all national stations were 0.235 and 0.285°C decade^{-1}, respectively. Therefore, the urbanization effect on the

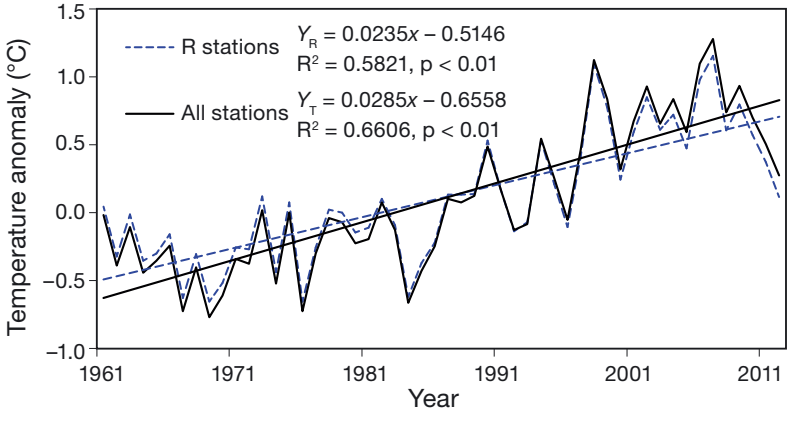

Fig. 4. Trends of surface air temperature (SAT) anomalies for R stations (i.e. stations with little or no urban impact) and all national stations in China during 1961–2012 . Y_R and Y_T indicate the linear fit of the average SAT series of R stations and all stations, respectively

Table 4. Urbanization effect on the change trends of surface air temperature (SAT) series in different sub-regions and China during 1961–2012. C_{LU}, C_{HU}, and C_T are the contributions of the urbanization effect to the overall SAT trend of LU, HU, and total stations, respectively (where LU and HU are stations with low and high urban impact, respectively). $^{**}p \leq 0.01$ (significance of each temperature trend was determined using a *t*-test)

Region	Temperature trend (°C decade^{-1})			Urbanization effect (°C decade^{-1})			Urbanization contribution (%)		
	$Trend_R$	$Trend_{LU}$	$Trend_{HU}$	$\Delta Trend_{LU}$	$\Delta Trend_{HU}$	$\Delta Trend_T$	C_{LU}	C_{HU}	C_T
S1	0.299**	0.343**	0.363**	0.044	0.064	0.046	13	18	13
S2	0.242**	0.29**	0.342**	0.048	0.100	0.051	17	29	17
S3	0.153**	0.175**	0.228**	0.022	0.075	0.030	13	33	16
S4	0.179**	0.241**	0.248**	0.062	0.069	0.045	26	28	20
S5	0.297**	0.374**	0.414**	0.077	0.117	0.056	21	28	16
China	0.235**	0.295**	0.325**	0.060	0.090	0.050	20	28	18

annual mean SAT trend of all national stations over China was estimated to be 0.05°C decade^{-1}.

The trends of HU stations ($Trend_{HU}$) were the highest in each sub-region, with high confidence levels, whereas the trends of R stations ($Trend_R$) were the lowest (Table 4). For example, in S1, changes in $Trend_R$, $Trend_{LU}$, and $Trend_{HU}$ were 0.299°C decade^{-1} ($p < 0.01$), 0.343°C decade^{-1} ($p < 0.01$), and 0.363°C decade^{-1} ($p < 0.01$), respectively. Obviously, varied urbanization biases were present in the SAT series observed by urban stations. Furthermore, urbanization effects on the regional average SAT trends obviously differed among the 5 sub-regions in China. The urbanization effect was lowest in S3, with a value of 0.022°C decade^{-1} for $\Delta Trend_{LU}$. However, for $\Delta Trend_{HU}$, the urbanization effect in S1 was lowest, with a value of 0.064°C decade^{-1}. The lowest magnitude of $\Delta Trend_T$ was also found in S3 (0.03°C decade^{-1}). In contrast, the largest magnitudes of $\Delta Trend_{LU}$, $\Delta Trend_{HU}$, and $\Delta Trend_T$ were estimated to be 0.077, 0.117, and 0.056°C decade^{-1} in S5, respectively. The contribution of urbanization to the overall warming of LU stations (C_{LU}) in S1, S2, and S3 was lower than 20%. However, the contribution of urbanization to the overall warming of HU stations (C_{HU}) in S2, S3, S4, and S5 was higher than 20%. Moreover, $\Delta Trend_{LU}$ and $\Delta Trend_{HU}$ were 0.06 and 0.09°C decade^{-1}, accounting for 20 and 28% of the overall warming trends, respectively.

4. DISCUSSION

4.1. Impact of UHI on SAT trends of urban stations

In the present study, we found that HU stations are significantly influenced by UHI, a result similar to that of previous studies (Portman 1993, Peterson & Vose 1997, Wang & Ge 2012, Wang et al. 2013). For instance, Hua et al. (2008) showed that the greatest urbanization warming (0.35°C) during 1961–2000 occurred in large city stations, approximately 0.088°C decade^{-1}; this was very similar to our estimation for HU stations (0.09°C decade^{-1}). Large cities have experienced rapid urbanization with intensive land-use change, which can strongly impact the surface energy balance (Li et al. 2017, 2018b). As a result, the stations in or close to large cities generally undergo faster warming than small-city stations (Liu 2009, Deng et al. 2015). The significant correlations between temperature trends and urban growth reported in previous studies further confirmed this phenomenon (He et al. 2013, Wang et al. 2017). However, the urbanization effect in the observed SAT series of urban stations is very local, and thus it should be precisely determined and eliminated before analyzing the regional temperature change.

4.2. Reasons for different estimates of urbanization biases

Existing estimates of the urbanization effect on observed temperature changes in China are significantly divergent (Zhang et al. 2010, Wang & Ge 2012, Jin et al. 2015, Ren et al. 2015). In addition to differences in study periods, different study areas may also lead to divergent estimates of urbanization biases due to the varied urbanization levels (Zhang et al. 2010). In general, a high urbanization level means a large influence of urbanization on SAT trends (He et al. 2013). However, we found that S1, with the largest EUI, had the lowest urbanization contribution among the 5 sub-regions (Table 4). One of the reasons is that the overall warming trend of S1 was higher than in other sub-regions. Moreover, inter-annual climate variability may contribute to the diversity of urbanization effects. For instance, Yao et al. (2017) sug-

gested that the inter-annual variations of UHI intensity were negatively correlated with land surface temperature, especially in northern China. We found that the urbanization effect in S5 was considerably larger than in S3, despite the background temperature trend of S5 being higher than that of S3 and their EUIs being the same. S5 (mainly containing Northwest China) is drier and colder than S3 (South China). Zhou et al. (2014) demonstrated that cities located in cold and dry regions have a larger UHI intensity than cities of the same size located in hot and humid regions. Thus, climatic condition is another reason for these diverse urbanization effects. All of these reasons highlight the necessity for division in the study of large-scale regions.

In addition to the above-mentioned factors, the different meteorological data used in previous studies are also among the primary reasons for different results (Wang & Yan 2016). For instance, inhomogeneous data may contain some uncertainties, such as the impact of station relocation on temperature records, which generally weaken the urbanization effect biases in the SAT series (Li et al. 2004a, Jin et al. 2015). In contrast, after homogenizing data based on the present locations of the stations, urbanization effect biases in the corrected SAT series of the stations that moved from urban areas to rural areas would be recovered (Cao et al. 2016). However, if some of these relocated stations are selected as rural stations, urbanization effects would be underestimated based on the homogenized data and UMR method. In this study, EUI was calculated by weighting an urban area within a wider buffer area (i.e. 30 km). Those relocated stations, being slighter farther away from urban areas, would be identified as urban stations again when their EUI became ≥1%. Thus, the above-mentioned uncertainties can be reduced to some extent.

Another important reason for different estimates is the varied study methods (Wang & Yan 2016). For instance, while He et al. (2013) found a large urbanization contribution (44.1%) by directly fitting the regression model between the SAT trend and urban growth around stations, Wang et al. (2017) detected a much smaller result (4%) by reducing background temperature change before applying this regression model. The results presented by He et al. (2013) may contain a large uncertainty induced by the background climate change. In contrast, the improved method used by Wang et al. (2017) should be better, which highlights the need to consider large-scale climate change when assessing local urban effects.

In general, background temperature change in large-scale regions can be explored based on the regional average temperature series generated from reanalysis data (Kalnay & Cai 2003, Wang et al. 2017) or observations of rural stations (Ren & Zhou 2014). However, some uncertainties may remain in the reanalysis data generated from numerical modeling and the observations generated from unevenly distributed rural stations (Simmons et al. 2004, Ren et al. 2015), resulting in variation among estimates. For instance, Wang & Yan (2015) found a very slight urban effect based on the OMR method (using ERA reanalysis data), but a dramatic urban warming (0.12°C decade^{-1}) based on the UMR method in the Beijing–Tianjin–Hebei metropolitan area. In contrast, Ren & Zhou (2014) showed that urbanization effects reached 0.047°C decade^{-1} during 1961–2008 in China, which was strikingly similar to our estimation (0.05°C decade^{-1}, see Table 4). This may be related to use of the same study method and climate dataset, as well as a similar study period.

Consequently, differences in data used and study methods are the main reasons for varied results (Wang & Yan 2016), which justifies the development of new methods, such as the method of selecting rural stations proposed in this study. The impact of choice of rural stations on estimates of urbanization biases is independently discussed in the next subsection.

4.3. Impact of choice of rural stations on estimates of urbanization bias

This study identified the R stations based on the magnitude of EUI, and found that the number of R stations in Southwest China and part of South China was far greater than in Northeast China and the coastal areas of East China. This is consistent with the results of Liao et al. (2017), who found few 'pure' rural stations in East China because of the high urbanization level and population density in this region. Selecting enough rural stations that are evenly distributed over the entire region is very important for calculating background temperature trends (Ren & Ren 2011). Thus, many researchers have had to select 'impure' rural stations located in small cities as reference stations (e.g. Li et al. 2004b, Xiong et al. 2010). Some rural stations identified in previous studies may have been converted to urban stations, resulting in an extreme lack of reference stations. As a specific example, Zengcheng station was identified as a HU station (EUI = 15%) in our study, but it had been previously treated as a rural station by Xiong et al. (2010).

The UHI can be detected even in small towns with populations of 10 000 or only a 1 km^2 urban area (Karl

et al. 1988, Heinl et al. 2015). Therefore, selecting rural stations with less representative regional climate conditions may underestimate urbanization warming (Jones & Lister 2009, Ge et al. 2013). For example, the urbanization effect estimated by Li et al. (2004b) (0.06°C during the last 50 yr) is substantially smaller than the results of Zhang et al. (2010) (0.076°C decade^{-1}) and of Ren et al. (2015) (0.074°C decade^{-1}). Li et al. (2004b) selected rural stations only based on population, which was less successful than the sophisticated procedures later adopted by Zhang et al. (2010) and Ren et al. (2015).

In addition to representativeness, spatial distribution of rural stations is another issue that should be considered. However, rural stations are unevenly distributed in China because of the imbalance of urbanization (Liao et al. 2017). Some previous studies arithmetically averaged all temperature records of rural stations in large-scale regions (e.g. Li et al. 2004b), which could not reflect the regional temperature changes (Jones & Hulme 1996). In contrast, in the present study, we adopted a grid-weighted method (Jones & Hulme 1996) to calculate the regional average temperature series. Thus, the uncertainties caused by uneven distribution of stations can be reduced when calculating large-scale patterns of temperature change (Zhang et al. 2010, Ren et al. 2015).

However, in this study, the lack and uneven distribution of rural stations still remains in some latitude–longitude grids. Moreover, a relaxed standard (EUI ≥ 2%) was used to select more rural stations in some regions due to rapid urbanization. All of these circumstances may also contribute to the diverse intensification of urbanization effects in different sub-regions. The urbanization contribution in China calculated in this study (18%) was smaller than the estimates of Zhang et al. (2010) (27.3%) and Ren et al. (2015) (24.9%). Thus, although we quantified the urban impact by considering urban areas and the distance from the station to the urban area, the current results should be considered as the lowest estimation.

4.4. Limitations of our approach and future outlook

Adopting NSL data to classify stations is a comparatively objective method and particularly useful in the periphery of urban areas (Owen et al. 1998). Our results are comparable with some recent studies (Yang et al. 2011, Ren & Zhou 2014, Jin et al. 2015). However, the method presented here still has limitations. For instance, although EUI quantified the impact of city size and distance from the city, some complicated microfactors related to UHI, such as density of built-up areas (Tran et al. 2006), urban fraction (Li et al. 2017), and surface imperviousness (Li et al. 2018b), were not considered. In addition, the lack of rural stations and their uneven distribution in some regions may lead to uncertainty in the results.

Recently, surface imperviousness (Li et al. 2018b) and urban fraction (Li et al. 2017) have been used as indicators linked to urbanization and UHI, which showed a promising method for selecting rural stations. Wang et al. (2017) applied linear regression between temperature trends induced by UHI and urban fraction trends to detect urbanization effects in China, which is another new way to study urbanization effects. Moreover, the impact of urbanization on the SAT trend should be different in different seasons because of the changes in natural climate factors, such as snow and rain (Li et al. 2016). Consequently, accurate accounts of urbanization biases based on new methods are still needed to improve the evaluation of temperature changes at different spatial and temporal scales.

5. CONCLUSIONS

In the present study, we adopted a method based on an index to classify stations in terms of the impact of urbanization. Urbanization biases in the average SAT series over China were then examined by comparing the regional average SAT series between urban (all stations) and rural stations. The main results are summarized as follows.

(1) The average trend of annual mean temperature over China during 1961–2012 was estimated to be up to 0.285°C decade^{-1}, ranging from 0.183°C decade^{-1} for S3 (South China) to 0.353°C decade^{-1} for S5 (Northwest China and a part of North China). However, there were spatial differences in the local temperature change that can be partly attributed to the significant urban impact on urban stations. The urbanization influence on temperature trends was effectively described by the EUI, which takes into account the urban area around a station and the station location relative to urbanized areas. With the help of the EUI, the 569 stations in China were classified into rural stations, stations with low urban impact, and stations with high urban impact. The index values for the last 2 groups were 2.6 and 15.3%, respectively.

(2) Significant urbanization effects on average temperature changes of urban stations were found all

over China. The average urbanization biases were estimated to be 0.06°C decade^{-1} for LU stations and 0.09°C decade^{-1} for HU stations, accounting for 20 and 28% of the overall warming, respectively.

(3) In the average SAT series of China, the urbanization effect was estimated to be 0.05°C decade^{-1} by contrasting the estimates from all stations and those from rural stations only. This effect accounted for 18% of the overall warming. Among the 5 sub-regions, the largest urbanization effect was detected in S5 (0.056°C decade^{-1}), whereas the smallest urbanization effect was detected in S3 (0.03°C decade^{-1}), which is located in South China. The diverse intensifications of urbanization effects in different sub-regions may be related to varied urbanization levels and different regional climates.

Acknowledgements. The study was financially supported by the National Nature Science Foundation of China (41771558), the National Key Research and Development Program of China (2016YFC0501707), the External Cooperation Program of BIC, Chinese Academy of Sciences (16146KYSB20150001), and the European Commission Programme Horizon 2020 project (635750). We thank Professor Deliang Chen of the University of Gothenburg for his helpful comments and suggestions.

LITERATURE CITED

Cao L, Zhu Y, Tang G, Yuan F, Yan Z (2016) Climatic warming in China according to a homogenized data set from 2419 stations. Int J Climatol 36:4384–4392

Chen XL, Zhao HM, Li PX, Yin ZY (2006) Remote sensing image-based analysis of the relationship between urban heat island and land use/cover changes. Remote Sens Environ 104:133–146

Chung U, Choi J, Yun JI (2004) Urbanization effect on the observed change in mean monthly temperatures between 1951–1980 and 1971–2000 in Korea. Clim Change 66:127–136

Deng X, Shi Q, Zhang Q, Shi C, Yin F (2015) Impacts of land use and land cover changes on surface energy and water balance in the Heihe River Basin of China, 2000–2010. Phys Chem Earth 79–82:2–10

Easterling DR, Peterson TC (1995) A new method for detecting and adjusting for undocumented discontinuities in climatological time series. Int J Climatol 15:369–377

Elvidge CD, Baugh KE, Dietz JB, Bland T, Sutton PC, Kroehl HW (1999) Radiance calibration of DMSP-OLS low-light imaging data of human settlements. Remote Sens Environ 68:77–88

Ge Q, Wang F, Luterbacher J (2013) Improved estimation of average warming trend of China from 1951–2010 based on satellite observed land-use data. Clim Change 121: 365–379

Hansen JE, Ruedy R, Sato M, Imhoff M and others (2001) A closer look at United States and global surface temperature change. J Geophys Res 106:23947–23963

Hartmann DL, Klein Tank AMG, Rusticucci M, Alexander LV and others (2013) Observations: atmosphere and surface. In: Stocker TF, Qin D, Plattner GK, Tignor MMB and others (eds) Climate change 2013: the physical science basis. Contribution of Working Group I to the Fifth Assessment Report of the IPCC. Cambridge University Press, Cambridge, p 31–39

He Y, Jia G, Hu Y, Zhou Z (2013) Detecting urban warming signals in climate records. Adv Atmos Sci 30:1143–1153

Heinl M, Hammerle A, Tappeiner U, Leitinger G (2015) Determinants of urban–rural land surface temperature differences — a landscape scale perspective. Landsc Urban Plan 134:33–42

Heldens W, Taubenböck H, Esch T, Heiden U, Wurm M (2013) Analysis of surface thermal patterns in relation to urban structure types: a case study for the city of Munich. Thermal infrared remote sensing. Springer, Netherlands

Holdaway MR (1996) Spatial modeling and interpolation of monthly temperature using kriging. Clim Res 6:215–225

Horel JD (1981) A rotated principal component analysis of the interannual variability of the Northern Hemisphere 500 mb height field. Mon Weather Rev 109:2080–2092

Hua LJ, Ma ZG, Guo WD (2008) The impact of urbanization on air temperature across China. Theor Appl Climatol 93:179–194

Imhoff ML, Lawrence WT, Stutzer DC, Elvidge CD (1997) A technique for using composite DMSP/OLS 'city lights' satellite data to map urban area. Remote Sens Environ 61:361–370

Jin K, Wang F, Chen D, Jiao Q, Xia L, Fleskens L, Mu X (2015) Assessment of urban effect on observed warming trends during 1955–2012 over China: a case of 45 cities. Clim Change 132:631–643

Jin K, Wang F, Li P (2018) Responses of vegetation cover to environmental change in large cities of China. Sustainability 10:270

Jones PD, Hulme M (1996) Calculating regional climatic time series for temperature and precipitation: methods and illustrations. Int J Climatol 16:361–377

Jones PD, Lister DH (2009) The urban heat island in Central London and urban-related warming trends in Central London since 1900. Weather 64:323–327

Jones PD, Groisman PY, Coughlan M, Plummer N, Wang WC, Karl TR (1990) Assessment of urbanization effects in time series of surface air temperature over land. Nature 347:171–177

Kaiser HF (1958) The varimax criterion for varimax rotation in factor analysis. Psychometrika 23:187–200

Kalnay E, Cai M (2003) Impact of urbanization and land-use change on climate. Nature 423:528–531

Karl TR, Diaz HF, Kukla G (1988) Urbanization: its detection and effect in the United States climate record. J Clim 1: 1099–1123

Khandelwal S, Goyal R, Kaul N, Singhal V (2011) Study of land surface temperature variations with distance from hot spots for urban heat island analysis. Geospatial World Forum, Theme Dimensions and Directions of Geospatial Industry, Hyderabad

Li H, Wang A, Guan D, Jin C, Wu J, Yuan F, Shi T (2016) Empirical model development for ground snow sublimation beneath a temperate mixed forest in Changbai mountain. J Hydrol Eng 21:04016040

Li H, Wolter M, Wang X, Sodoudi S (2017) Impact of land cover data on the simulation of urban heat island for Berlin using WRF coupled with bulk approach of Noah-LSM. Theor Appl Climatol 6:1–15

Li H, Meier F, Lee X, Chakraborty T, Liu J, Schaap M, Sodoudi S (2018a) Interaction between urban heat island and urban pollution island during summer in Berlin. Sci Total Environ 636:818–828

Li H, Zhou Y, Li X, Meng L, Wang X, Wu S, Sodoudi S (2018b) A new method to quantify surface urban heat island intensity. Sci Total Environ 624:262–272

Li Q, Liu X, Zhang H, Peterson TC, Easterling DR (2004a) Detecting and adjusting temporal inhomogeneity in Chinese mean surface air temperature data. Adv Atmos Sci 21:260–268

Li Q, Zhang H, Liu X, Huang J (2004b) Urban heat island effect on annual mean temperature during the last 50 years in China. Theor Appl Climatol 79:165–174

Li Y, Zhu L, Zhao X, Li S, Yan Y (2013) Urbanization impact on temperature change in China with emphasis on land cover change and human activity. J Clim 26:8765–8780

Liao W, Wang D, Liu X, Wang G, Zhang J (2017) Estimated influence of urbanization on surface warming in Eastern China using time-varying land use data. Int J Climatol 37:3197–3208

Liu Y (2009) Exploring the relationship between urbanization and energy consumption in China using ARDL (autoregressive distributed lag) and FDM (factor decomposition model). Energy 34:1846–1854

Liu Z, He C, Zhang Q, Huang Q, Yang Y (2012) Extracting the dynamics of urban expansion in China using DMSP-OLS nighttime light data from 1992 to 2008. Landsc Urban Plan 106:62–72

Mohsin T, Gough WA (2012) Characterization and estimation of urban heat island at Toronto: impact of the choice of rural sites. Theor Appl Climatol 108:105–117

Owen TW, Gallo KP, Elvidge CD, Baugh KE (1998) Using DMSP-OLS light frequency data to categorize urban environments associated with US climate observing station. Int J Remote Sens 19:3451–3456

Peterson TC (2003) Assessment of urban versus rural in situ surface temperatures in the contiguous United States: no difference found. J Clim 16:2941–2959

Peterson TC, Vose RS (1997) An overview of the global historical climatology network temperature database. Bull Am Meteorol Soc 78:2837–2849

Portman DA (1993) Identifying and correcting urban bias in regional time series: surface temperature in China's northern plains. J Clim 6:2298–2308

Ren G, Zhou Y (2014) Urbanization effect on trends of extreme temperature indices of national stations over mainland China, 1961–2008. J Clim 27:2340–2360

Ren G, Zhou Y, Chu Z, Zhou J, Zhang A, Guo J, Liu X (2008) Urbanization effects on observed surface air temperature trends in North China. J Clim 21: 1333–1348

Ren G, Li J, Ren Y, Chu Z and others (2015) An integrated procedure to determine a reference station network for evaluating and adjusting urban bias in surface air temperature data. J Appl Meteorol Climatol 54:1248–1266

Ren Y, Ren G (2011) A remote-sensing method of selecting reference stations for evaluating urbanization effect on surface air temperature trends. J Clim 24:3179–3189

Simmons AJ, Jones PD, da Costa Bechtold V, Beljaars ACM and others (2004) Comparison of trends and low-frequency variability in CRU, ERA-40, and NCEP/NCAR analyses of surface air temperature. J Geophys Res 109: D24115

Tayanç M, Toros H (1997) Urbanization effects on regional climate change in the case of four large cities of Turkey. Clim Change 35:501–524

Tran H, Uchihama D, Ochi S, Yasuoka Y (2006) Assessment with satellite data of the urban heat island effects in Asian mega cities. Int J Appl Earth Obs Geoinf 8:34–48

Trenberth KE (2004) Climatology (communication arising): rural land-use change and climate. Nature 427:213–214

Wang F, Ge Q (2012) Estimation of urbanization bias in observed surface temperature change in China from 1980 to 2009 using satellite land-use data. Chin Sci Bull 57:1708–1715

Wang F, Ge Q, Wang S, Li Q, Jones PD (2015) A new estimation of urbanization's contribution to the warming trend in China. J Clim 28:8923–8938

Wang J, Yan ZW (2016) Urbanization-related warming in local temperature records: a review. Atmos Ocean Sci Lett 9:129–138

Wang J, Yan ZW, Zhen L, Liu WD, Yang YC (2013) Impact of urbanization on changes in temperature extremes in Beijing during 1978–2008. Chin Sci Bull 58:4679–4686

Wang J, Tett SFB, Yan Z (2017) Correcting urban bias in large-scale temperature records in China, 1980–2009. Geophys Res Lett 44:401–408

Wang M, Yan X (2015) A comparison of two methods on the climatic effects of urbanization in the Beijing-Tianjin-Hebei metropolitan area. Adv Meteorol 2015:352360

Winkler JA, Skaggs RH, Baker DG (1981) Effect of temperature adjustments on the Minneapolis-St. Paul urban heat island. J Appl Meteorol 20:1295–1300

Xiong Y, Zhang Z, Chen F, Wang R (2010) Estimation of urbanization effect on climatic warming over the recent 30 years in Guangzhou, south China. 18th International Conference on Geoinformatics: Geoscience in Change, Geoinformatics. June 2010. Peking University, Beijing

Yang X, Hou Y, Chen B (2011) Observed surface warming induced by urbanization in east China. J Geophys Res Atmos 116:D14113

Yang YJ, Wu BW, Shi CE, Zhang JH and others (2013) Impacts of urbanization and station-relocation on surface air temperature series in Anhui province, China. Pure Appl Geophys 170:1969–1983

Yao R, Wang L, Huang X, Niu Z, Liu F, Wang Q (2017) Temporal trends of surface urban heat islands and associated determinants in major Chinese cities. Sci Total Environ 609:742–754

Zhang AY, Ren GY, Zhou JX, Chu ZY, Ren YY, Tang GL (2010) On the urbanization effect on surface air temperature trends over China. Acta Meteorol Sin 68:957–966 (in Chinese)

Zhou D, Zhao S, Liu S, Zhang L, Zhu C (2014) Surface urban heat island in China's 32 major cities: spatial patterns and drivers. Remote Sens Environ 152:51–61

Zhou Y, Ren G (2011) Change in extreme temperature event frequency over mainland China, 1961–2008. Clim Res 50:125–139

Appendix. Example of homogeneity adjustment for temperature series

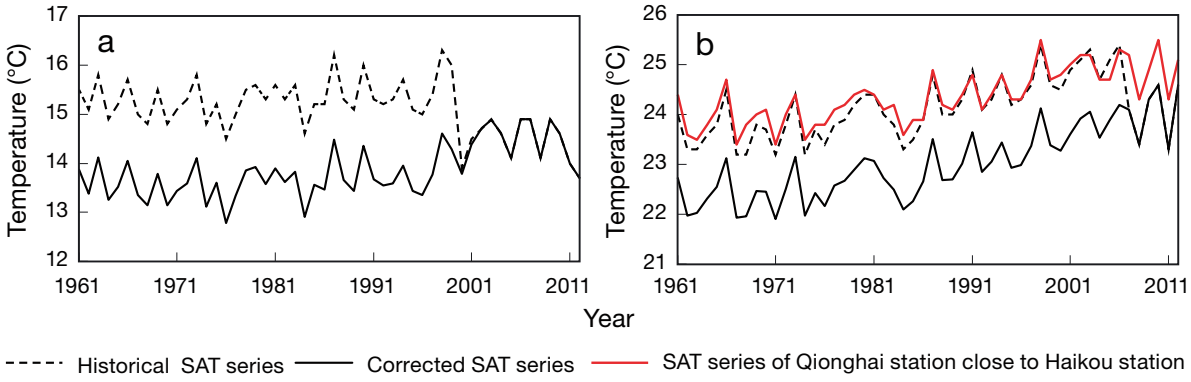

Fig. A1. Annual mean surface air temperature (SAT) time series of (a) Guiyang station and (b) Haikou station before (dashed curve) and after (solid curve) adjustment

Explanation for the homogeneity adjustment

Here we show Guiyang and Haikou stations as examples to illustrate the adjustment of connected SAT series (Fig. A1). For Guiyang station, 1 obvious discontinuous point caused by relocation in 1999 (dashed curve) was adjusted in the CHHT dataset (solid curve between 1961 and 2004). The adjusted data series during 1961–2004 was connected to the records after 2004 (Fig. A1a). Due to Guiyang station not being relocated after 2004, the connected SAT series did not need to be adjusted further. Similarly, 1 obvious discontinuous point caused by relocation in 2007 was detected in the connected SAT series of Haikou station (Fig. A1b). Therefore, the 1961–2006 records (dashed curve) were adjusted based on the SAT series of Qionghai station which was close to Haikou station and had never been relocated. After connection, rechecking, and adjustment, the homogeneities and continuities of the SAT series during 1961–2012 are comparatively reasonable.

Editorial responsibility: Eduardo Zorita, Geesthacht, Germany

Submitted: November 1, 2017; Accepted: July 9, 2018
Proofs received from author(s): August 29, 2018